Subleading contributions to the chiral three-nucleon force: Long-range terms

V. Bernard,[1,*] E. Epelbaum,[2,3,†] H. Krebs,[3,‡] and Ulf-G. Meißner[3,2,§]

[1]*Université Louis Pasteur, Laboratoire de Physique Théorique 3-5, rue de l'Université, F-67084 Strasbourg, France*

[2]*Forschungszentrum Jülich, Institut für Kernphysik (Theorie), D-52425 Jülich, Germany*

[3]*Universität Bonn, Helmholtz-Institut für Strahlen-und Kernphysik (Theorie), D-53115 Bonn, Germany*

(Received 16 December 2007; published 25 June 2008)

We derive the long-range contributions to the tree-nucleon force at next-to-next-to-next-to-leading order in the chiral expansion. We give both momentum- and coordinate-space representations.

DOI: 10.1103/PhysRevC.77.064004 PACS number(s): 13.75.Cs, 21.30.−x

I. INTRODUCTION

Three-nucleon forces (3NFs) are an indispensable ingredient in accurate few-nucleon and nuclear structure calculations. In particular, the three-nucleon system shows clear evidence for 3NFs (see the recent general introduction [1]). Chiral effective field theory is the appropriate tool to analyze nuclear forces. Precise two-nucleon potentials have been developed at next-to-next-to-next-to-leading order (N^3LO) in the chiral expansion (see Refs. [2,3]). Three-nucleon forces first appear at N^2LO in the Weinberg counting scheme [4,5] and have been analyzed and scrutinized in Refs. [6–11]. There are various reasons for improving the theoretical precision of these 3NFs: 1. One should utilize the two- and three-nucleon forces at the same order in the expansion. 2. There are some outstanding discrepancies between theory and experiment such as, for example, the recently measured differential cross section in deuteron breakup at low energies [12] or the long-standing A_y puzzle [13,14]. 3. The theoretical uncertainty employing only the leading 3NFs quickly grows with increasing energy if one investigates, for example, nucleon-deuteron scattering or breakup. It is therefore timely and necessary to derive the chiral 3NF at N^3LO. In this work, we focus our attention on the long-range contributions at this order, which are free of unknown coupling constants. Here, we consider the chiral effective Lagrangian with pions and nucleons. The precise relation of the results presented here to an effective field theory also including spin-3/2 degrees of freedom will be the subject of a subsequent paper.

As we will show later, there are five different topologies contributing to the 3NF at N^3LO. From these, three topologies make up the long-range contribution, which is defined by not including any multinucleon contact interactions. This long-range part is given by two-pion (2π) exchange graphs, two-pion-one-pion (2π-1π) exchange graphs, and the so-called ring diagrams, where the pion loop connects all three nucleon lines. The first type of graph has recently been considered based on the so-called infrared regularization in Ref. [15], we will compare our results to that work in the following. The spin-isospin structures originating from ring diagrams with one explicit delta intermediate state have been incorporated in the Illinois 3NF model [16]. Earlier, Coon and Friar [17] systematically constructed the $1/m$ (with m the nucleon mass) corrections to the 2π exchange 3NF, and the so-called drift effects resulting from the boost of the two-nucleon force were worked out in Ref. [18]. We will compare to these works in our subsequent paper, where we discuss the shorter ranged part of the 3NF at this order and the corresponding $1/m$ corrections. Notice further that ring diagrams have already been studied in the pioneering work of Ref. [19]. As the authors of this work concentrated mainly on the contributions from the P_{33} πN partial wave, a direct comparison with their results is only meaningful by using an effective field theory with explicit delta degrees of freedom. In addition, the authors of Ref. [19] do not provide the momentum-space expressions and do not explicitly carry out the spin-isospin algebra.

This manuscript is organized as follows. In Sec. II we first write down the effective chiral Lagrangian and discuss the general structure of the 3NF at N^3LO. In the subsequent Secs. II A, II B, and II C we give our results for the 2π, 2π-1π, and ring graphs, respectively, both in momentum- and coordinate-space representations. We end with a summary and conclusions in Sec. III. In particular, we make some comments on the 3NF arising in an extension of this work with explicit delta degrees of freedom. The lengthy expressions for the momentum-space representation of the ring diagrams are relegated to the Appendix.

II. LONG-RANGE CONTRIBUTIONS TO THE 3NF AT N^3LO

The calculations performed in the following are based on the effective chiral Lagrangian for pions and nucleons. We employ here the heavy-baryon formulation and display only the terms of relevance for our study:

$$\begin{aligned}
\mathcal{L} &= \mathcal{L}^{\Delta=0} + \mathcal{L}^{\Delta=1} + \mathcal{L}^{\Delta=2} + \cdots, \\
\mathcal{L}^{\Delta=0} &= \frac{F^2}{4}\langle \nabla^\mu U \nabla_\mu U^\dagger + \chi_+\rangle + \bar{N}\,(iv\cdot D + g_A u\cdot S)\,N \\
&\quad + \ldots, \\
\mathcal{L}^{\Delta=1} &= \bar{N}\left(c_1\langle\chi_+\rangle + c_2(v\cdot u)^2 + c_3 u\cdot u \right. \\
&\quad \left. + c_4[S^\mu, S^\nu]u_\mu u_\nu\right) N + \ldots, \\
\mathcal{L}^{\Delta=2} &= \bar{N}\left(d_{16} S\cdot u\langle\chi_+\rangle + i d_{18} S^\mu [D_\mu, \chi_-] \right. \\
&\quad \left. + \tilde{d}_{28}(i\langle\chi_+\rangle v\cdot D + \text{h.c.}) + \ldots\right) N + \ldots,
\end{aligned} \tag{2.1}$$

*bernard@lpt6.u-strasbg.fr
†e.epelbaum@fz-juelich.de
‡hkrebs@itkp.uni-bonn.de
§meissner@itkp.uni-bonn.de; www.itkp.uni-bonn.de

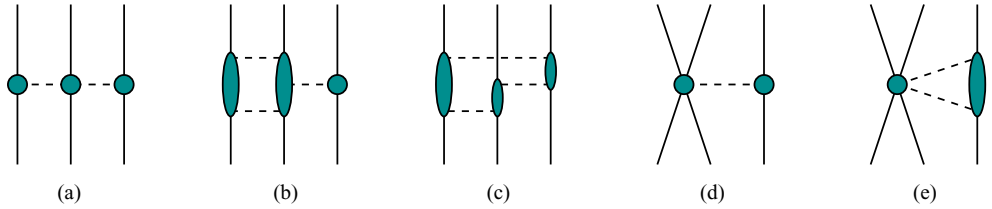

FIG. 1. (Color online) Various topologies that appear in the 3NF at N^{3}LO. Solid and dashed lines represent nucleons and pions, respectively. Shaded blobs are the corresponding amplitudes. The long-range part of the 3NF considered in this paper consists of (a) 2π exchange graphs, (b) 2π-1π diagrams, and (c) the so-called ring diagrams. The topologies (d) and (e) involve four-nucleon contact operators and are considered of shorter range.

where the c_i are low-energy constants and N, v_μ, and S_μ denote the large component of the nucleon field, the nucleons four-velocity, and the covariant spin vector, respectively. We use standard notation: $U(x) = u^2(x)$ collects the pion fields, $u_\mu = i(u^\dagger \partial_\mu u - u \partial_\mu u^\dagger)$, $\chi_+ = u^\dagger \chi u^\dagger + u \chi^\dagger u$ includes the explicit chiral symmetry breaking resulting from the finite light quark masses, $\langle \ldots \rangle$ denotes a trace in flavor space, and D_μ is the chiral covariant derivative for the nucleon field. Notice further that the first terms in the expansion of $U(\pi)$ in powers of the pion fields read

$$U(\boldsymbol{\pi}) = 1 + \frac{i}{F_\pi}\boldsymbol{\tau}\cdot\boldsymbol{\pi} - \frac{1}{2F_\pi^2}\boldsymbol{\pi}^2 - \frac{i\alpha}{F_\pi^3}(\boldsymbol{\tau}\cdot\boldsymbol{\pi})^3 + \frac{8\alpha - 1}{8F_\pi^4}\boldsymbol{\pi}^4 + \cdots, \tag{2.2}$$

where $\boldsymbol{\tau}$ denote the Pauli isospin matrices and α is an arbitrary constant. For further notation and discussion, we refer to Ref. [20]; a recent review is given in Ref. [21]. Following Weinberg [4,5], we define the dimension Δ of the Lagrangian via

$$\Delta = d + \tfrac{1}{2}n - 2, \tag{2.3}$$

where d and n are the number of derivatives or insertions of the pion mass M_π and nucleon field operators, respectively. The pertinent low-energy constants (LECs) of the leading-order effective Lagrangian are the nucleon axial-vector coupling g_A and the pion decay constant F_π. Notice that although all couplings and masses appearing in the effective Lagrangian should, strictly speaking, be taken at their SU(2) chiral limit values, to the accuracy we are working, we can use their pertinent physical values. In addition, we have the LECs d_{16}, d_{18}, and $\tilde{d}_{28}$ from the πN Lagrangian at order $\Delta = 2$. The ellipses in the parentheses in the last line of Eq. (2.1) refer to terms proportional to the LECs $d_{1,2,3,5,14,15}$ and $\tilde{d}_{24,26,27,28,30}$, which generate $\pi\pi NN$ vertices [20] but do not contribute to the 3NF at N^{3}LO as will be shown later. We also omit in Eq. (2.1) pion vertices with $\Delta = 2$ and proportional to the LECs $l_{3,4}$, which do not show up explicitly in the formulation based on renormalized pion fields at the considered order; see Ref. [22] for more details.

For a connected N-nucleon diagram with L loops and V_i vertices of dimension Δ_i, the irreducible contribution[1] to the scattering amplitude scales as Q^ν, where Q is a generic low-momentum scale associated with external nucleon three-momenta or M_π and

$$\nu = -4 + 2N + 2L + \sum_i V_i \Delta_i. \tag{2.4}$$

Consequently, at N^{3}LO, which corresponds to $\nu = 4$, one needs to take into account two classes of connected diagrams: tree diagrams with one insertion of the $\Delta = 2$ interactions and one-loop graphs involving only lowest order vertices with $\Delta = 0$. Notice that it is not possible to draw $3N$ diagrams with two insertions of $\Delta = 1$ vertices at this order. We further emphasize that similar to the case of the leading four-nucleon force considered in Refs. [23,24], disconnected diagrams lead to vanishing contributions to the 3NF and will not be discussed in what follows.

The structure of the 3NF at N^{3}LO is visualized in Fig. 1 and can be written as

$$V_{3\mathrm{N}}^{(4)} = V_{2\pi}^{(4)} + V_{2\pi\text{-}1\pi}^{(4)} + V_{\mathrm{ring}}^{(4)} + V_{1\pi\text{-cont}}^{(4)} + V_{2\pi\text{-cont}}^{(4)} + V_{1/m}^{(4)}. \tag{2.5}$$

Whereas the 2π-1π, ring, and two-pion-exchange-contact (2π-cont) topologies start to contribute at N^{3}LO, the 2π and one-pion-exchange-contact (1π-cont) graphs already appear at N^{2}LO, yielding the following contributions to the 3NF [6,8]:

$$\begin{aligned} V_{2\pi}^{(3)} &= \frac{g_A^2}{8F_\pi^4}\,\frac{\vec{\sigma}_1\cdot\vec{q}_1\;\vec{\sigma}_3\cdot\vec{q}_3}{\left[q_1^2 + M_\pi^2\right]\left[q_3^2 + M_\pi^2\right]} \\ &\quad\times\left[\boldsymbol{\tau}_1\cdot\boldsymbol{\tau}_3\left(-4c_1M_\pi^2 + 2c_3\vec{q}_1\cdot\vec{q}_3\right) + c_4\boldsymbol{\tau}_1\times\boldsymbol{\tau}_3\cdot\boldsymbol{\tau}_2\;\vec{q}_1\times\vec{q}_3\cdot\vec{\sigma}_2\right], \\ V_{1\pi\text{-cont}}^{(3)} &= -\frac{g_A D}{8F_\pi^2}\,\frac{\vec{\sigma}_3\cdot\vec{q}_3}{q_3^2 + M_\pi^2}\;\boldsymbol{\tau}_1\cdot\boldsymbol{\tau}_3\;\vec{\sigma}_1\cdot\vec{q}_3, \end{aligned} \tag{2.6}$$

where the subscripts refer to the nucleon labels and $\vec{q}_i = \vec{p}\,'_i - \vec{p}_i$, with $\vec{p}\,'_i$ and $\vec{p}_i$ being the final and initial momenta of the nucleon i. Further, $q_i \equiv |\vec{q}_i|$, σ_i denote the Pauli spin matrices, and D refers to the low-energy constant accompanying the leading $\pi NNNN$ vertex. Here and throughout this work, the results are always given for a particular choice of nucleon labels. The full expression for the 3NF results by taking into account all possible permutations of the nucleons,[2] that is,

$$V_{3N}^{\mathrm{full}} = V_{3N} + \text{all permutations}. \tag{2.7}$$

[1] This is the contribution that is not generated through iterations in the dynamical equation and that gives rise to the nuclear force.

[2] For three nucleons there are altogether six permutations.

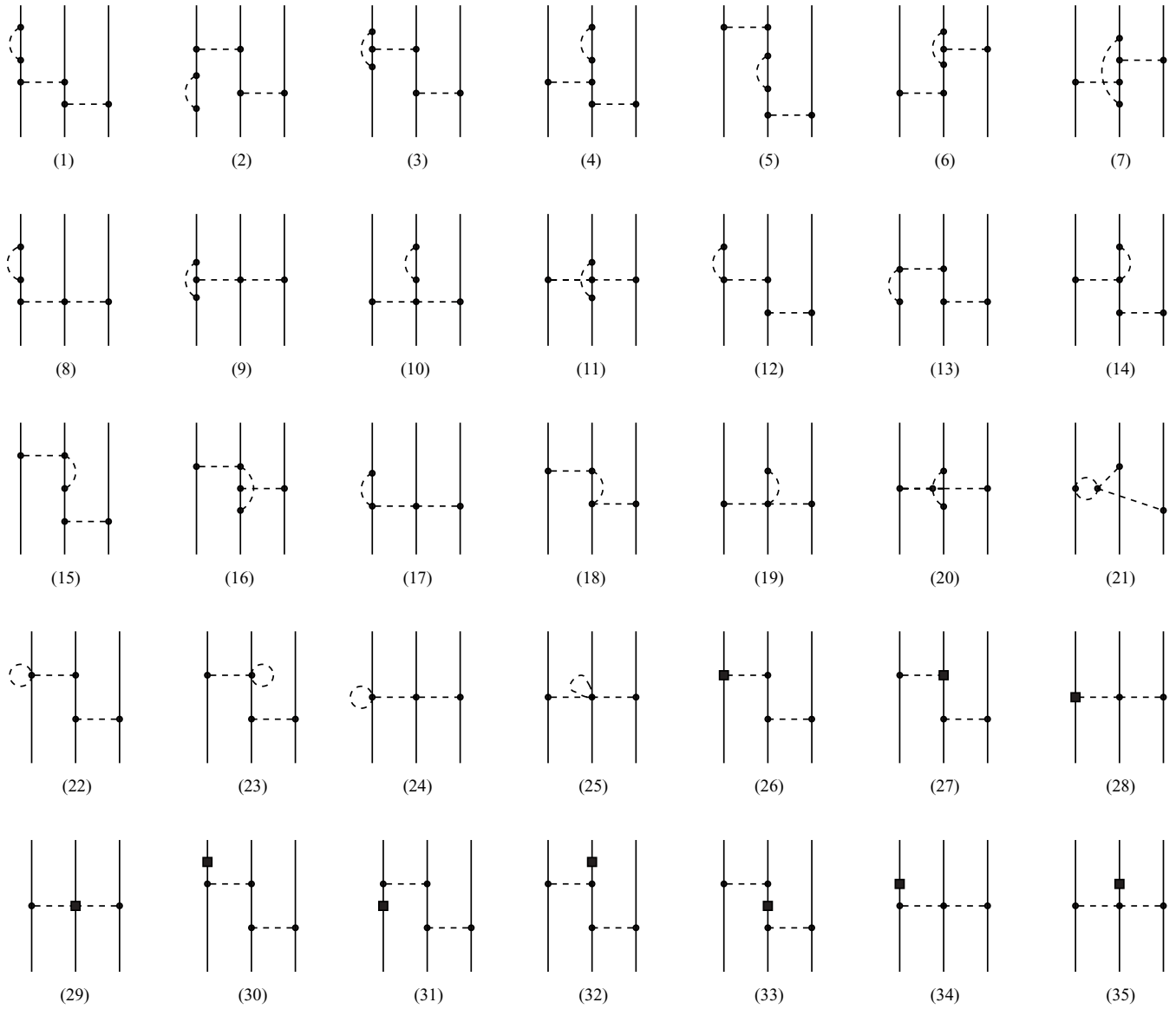

FIG. 2. Two-pion exchange $3N$ diagrams at N^{3}LO. Solid dots (filled rectangles) denote vertices of dimension $\Delta_i = 0$ ($\Delta_i = 2$). Diagrams that result from the interchange of the nucleon lines and/or application of the time-reversal operation are not shown. For remaining notation see Fig. 1.

In this work, we focus on the long-range contributions $V_{2\pi}^{(4)}$, $V_{2\pi\text{-}1\pi}^{(4)}$, and $V_{\text{ring}}^{(4)}$ resulting from diagrams (a), (b), and (c) in Fig. 1, respectively. The remaining terms resulting from graphs (d) and (e) in Fig. 1 and the relativistic $1/m$ corrections will be discussed separately.

A. Two-pion exchange topology

The 2π exchange diagrams at $\nu = 4$ corresponding to topology (a) of Fig. 1 are depicted in Fig. 2. We do not show graphs involving tadpoles at pion lines, which just renormalize the pion field and mass (see Ref. [22] for details). A close inspection of the diagrams in Fig. 2 shows that most of them do not generate 3NFs. First, the contribution from graphs (12)–(17) involves an odd power of the loop momentum $\vec{l}$ to be integrated over and thus vanishes. Second, diagrams (1), (2), (4), (8), (10), (30)–(32), (34), and (35) just renormalize the external nucleon legs. Similarly, Feynman diagrams (3), (9), (22)–(24), and (26)–(28) lead to renormalization of the leading pion-nucleon coupling without producing any new structures. All these contributions are taken into account by replacing the bare LECs in the leading 2π exchange $3N$ scattering amplitude by renormalized ones. This suggests that there are no N^{3}LO corrections to the 3NF from these graphs since the 2π exchange $3N$ diagrams at order $\nu = 2$ do not generate any nonvanishing 3NF. Given the fact that nuclear potentials are, in general, not uniquely defined, this argument based on the (on-shell) scattering amplitude should be taken with care. We have, however, verified that this is indeed the case by explicitly calculating the corresponding 3NF using the method of unitary transformation along the

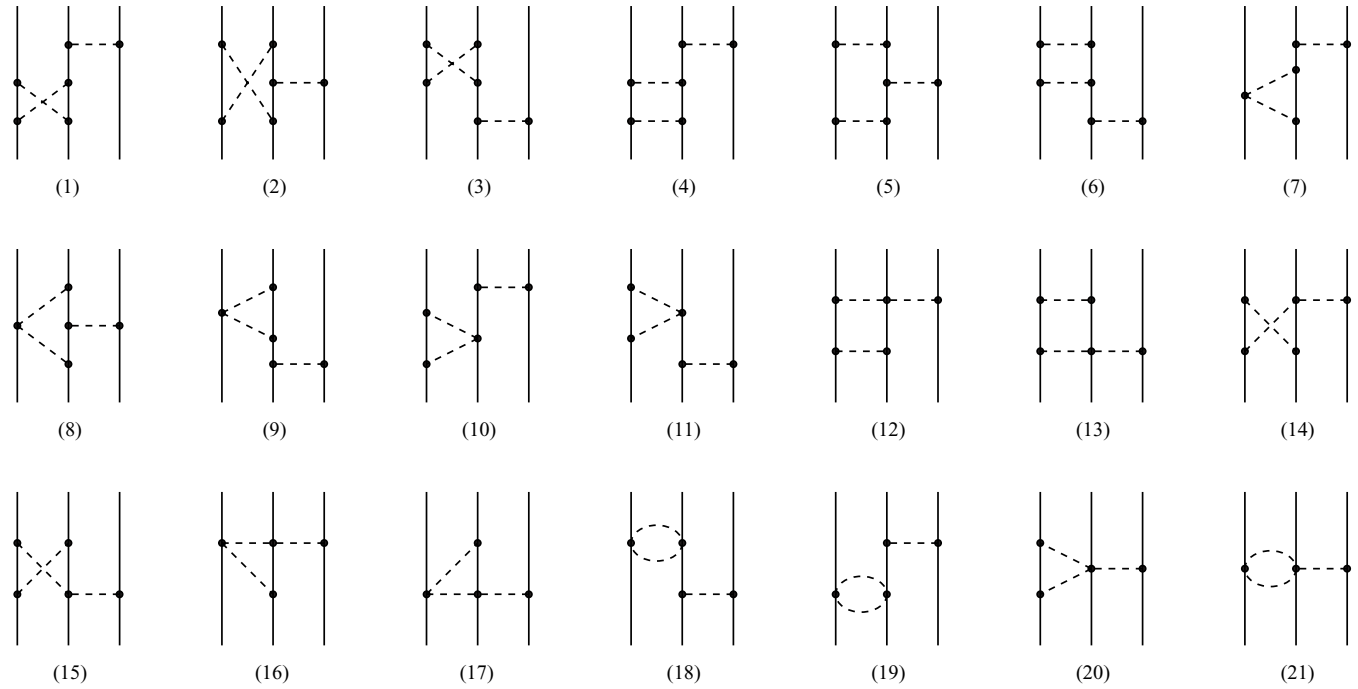

FIG. 3. 2π-1π diagrams at N^{3}LO. Graphs resulting from the interchange of the nucleon lines are not shown. For notation see Figs. 1 and 2.

lines of Ref. [24]. From the remaining graphs in Fig. 2, diagram (11) does not contribute at the considered order owing to the $1/m$ suppression caused by the time derivative entering the Weinberg-Tomozawa vertex.[3] For the same reason, diagram (25) also leads to a vanishing result at the order considered. Here, the time derivative acts either on the pions exchanged between two nucleons, leading to a $1/m$ suppression, or on the pion in the tadpole, giving an odd power of the loop momentum l^0 to be integrated over. Further, it is easy to see that Feynman diagrams (18) and (21) also do not contribute. Diagram (29) involves one insertion of the $\pi\pi NN$ vertices of dimension $\nu = 2$. The relevant vertices are proportional to the LECs $d_{1,2,3,5,14,15}$ and $\tilde{d}_{24,26,27,28,30}$. The corresponding 3NF is shifted to higher orders since all these vertices involve at least one time derivative (see Ref. [20] for explicit expressions). Last but not least, we also found that diagram (33) does not generate any 3NF. Thus, we are left with diagrams (5)–(7), (19), and (20). The 3NF contribution from diagrams (5)–(7) can be evaluated straightforwardly by using the expressions for the effective Hamilton operator from Ref. [24]. Diagrams (19) and (20) do not involve reducible topologies and can be evaluated by using the Feynman graph technique. Notice that the individual contributions from graphs (19) and (20) in Fig. 2 and from diagram (20) in Fig. 3 depend on the arbitrary constant α, which specifies the parametrization of the matrix U [see Eq. (2.2)]. Clearly, their sum is α-independent.

[3]This graph does not involve reducible time-ordered topologies. Its contribution to the nuclear force is, therefore, most easily obtained by using the Feynman graph technique. The $1/m$ suppression from the time derivative entering the Weinberg-Tomozawa vertex follows then simply from the four-momentum conservation.

We are now in the position to present our results. The expressions for diagrams (5)–(7) and (19) can be cast into the form of Eq. (2.6), leading only to shifts in the values of the LECs c_i:

$$c_1 \to \bar{c}_1 = c_1 - \frac{g_A^2\, M_\pi}{64\pi\, F_\pi^2}, \quad c_3 \to \bar{c}_3 = c_3 + \frac{g_A^4\, M_\pi}{16\pi\, F_\pi^2},$$
$$c_4 \to \bar{c}_4 = c_4 - \frac{g_A^4\, M_\pi}{16\pi\, F_\pi^2}, \tag{2.8}$$

with $\delta c_1 = -0.13\ \text{GeV}^{-1}$ and $\delta c_3 = -\delta c_4 = 0.52\ \text{GeV}^{-1}$. These shifts are of the order of 20% to 30% of the corresponding LECs and thus cannot be neglected in precision studies of 3NFs. In contrast to this, the contribution from graph (20) takes a more complicated form compared to Eq. (2.6) and is given by

$$\begin{aligned} V_{2\pi}^{(4)} = {} & \frac{g_A^4}{256\pi\, F_\pi^6}\, \frac{\vec{\sigma}_1\cdot\vec{q}_1\ \vec{\sigma}_3\cdot\vec{q}_3}{\big[q_1^2+M_\pi^2\big]\big[q_3^2+M_\pi^2\big]} \\ & \times \Big[\boldsymbol{\tau}_1\cdot\boldsymbol{\tau}_3\big(M_\pi\big(M_\pi^2+3q_1^2+3q_3^2+4\vec{q}_1\cdot\vec{q}_3\big) \\ & + \big(2M_\pi^2+q_1^2+q_3^2+2\vec{q}_1\cdot\vec{q}_3\big) \\ & \times \big(3M_\pi^2+3q_1^2+3q_3^2+4\vec{q}_1\cdot\vec{q}_3\big)A(q_2)\big) \\ & - \boldsymbol{\tau}_1\times\boldsymbol{\tau}_3\cdot\boldsymbol{\tau}_2\ \vec{q}_1\times\vec{q}_3\cdot\vec{\sigma}_2 \\ & \times \big(M_\pi + (4M_\pi^2+q_1^2+q_3^2+2\vec{q}_1\cdot\vec{q}_3)A(q_2)\big)\Big]. \end{aligned} \tag{2.9}$$

Here, we have used dimensional regularization to evaluate the loop integrals. In this framework, the loop function $A(q)$ is given by

$$A(q) = \frac{1}{2q}\arctan\frac{q}{2M_\pi}. \tag{2.10}$$

We further emphasize that these expressions correspond to the choice $\alpha = 0$. Notice also that some pieces in Eq. (2.9) can be brought into a form corresponding to the 2π-1π and 2π-cont topologies by canceling out the pion propagators with terms in the numerator. The 2π exchange contributions arising from diagrams in Fig. 2 have also been considered recently by Ishikawa and Robilotta based on the infrared regularization [15]. We have verified that the long-range 2π exchange contributions in Eqs. (2.6), (2.8), and (2.9) agree with the ones given in Ref. [15] provided the latter are expanded in powers of $1/m$ and the leading terms are kept.

The coordinate-space representation of the 2π exchange 3NF can be obtained in a straightforward way. For the leading terms in the first line of Eq. (2.6) and the corrections in Eq. (2.8) one gets

$$\begin{aligned} &V_{2\pi}(\vec{r}_{12},\vec{r}_{32}) \\ &= \int \frac{d^3q_1}{(2\pi)^3}\frac{d^3q_3}{(2\pi)^3} e^{i\vec{q}_1\cdot\vec{r}_{12}}\, e^{i\vec{q}_3\cdot\vec{r}_{32}}\, V_{2\pi}(\vec{q}_1,\vec{q}_3) \\ &= \frac{g_A^2 M_\pi^6}{128\pi^2 F_\pi^4}\, \vec{\sigma}_1\cdot\vec{\nabla}_{12}\, \vec{\sigma}_3\cdot\vec{\nabla}_{32}[\boldsymbol{\tau}_1\cdot\boldsymbol{\tau}_3(4\bar{c}_1 + 2\bar{c}_3\vec{\nabla}_{12}\cdot\vec{\nabla}_{32}) \\ &\quad + \bar{c}_4\boldsymbol{\tau}_1\times\boldsymbol{\tau}_3\cdot\boldsymbol{\tau}_2\, \vec{\nabla}_{12}\times\vec{\nabla}_{32}\cdot\vec{\sigma}_2]U_1(x_{12})\, U_1(x_{32}), \end{aligned} \tag{2.11}$$

where $\vec{r}_{ij} \equiv \vec{r}_i - \vec{r}_j$ is the distance between the nucleons i and j, the $\vec{x}_i \equiv M_\pi \vec{r}_i$ are dimensionless distances, the $\vec{\nabla}_i$ act on $\vec{x}_i$, and $x_{ij} \equiv |\vec{x}_{ij}|$. Further, the scalar function $U_1(x)$ is defined as

$$U_1(x) = \frac{4\pi}{M_\pi}\int \frac{d^3q}{(2\pi)^3}\frac{e^{i\vec{q}\cdot\vec{x}/M_\pi}}{q^2+M_\pi^2} = \frac{e^{-x}}{x}. \tag{2.12}$$

Similarly, for the terms in Eq. (2.9) that do not involve the loop function $A(q_2)$, one obtains

$$\begin{aligned} &V_{2\pi}(\vec{r}_{12},\vec{r}_{32}) \\ &= \frac{g_A^4 M_\pi^7}{4096\pi^3 F_\pi^6}\vec{\sigma}_1\cdot\vec{\nabla}_{12}\, \vec{\sigma}_3\cdot\vec{\nabla}_{32}\big[\boldsymbol{\tau}_1\cdot\boldsymbol{\tau}_3\big(-1+3\nabla_{12}^2 \\ &\quad + 3\nabla_{32}^2 + 4\vec{\nabla}_{12}\cdot\vec{\nabla}_{32}\big) - \boldsymbol{\tau}_1\times\boldsymbol{\tau}_3\cdot\boldsymbol{\tau}_2\, \vec{\nabla}_{12}\times\vec{\nabla}_{32}\cdot\vec{\sigma}_2\big] \\ &\quad \times U_1(x_{12})\, U_1(x_{32}). \end{aligned} \tag{2.13}$$

It should be understood that the obtained expressions are only valid in the region of space where the interparticle distances are large (i.e., larger than the inverse pion mass). The behavior of the potential at shorter distances is, in general, affected by the regularization procedure, which is not considered in the present work.

To obtain the coordinate-space representation for the terms in Eq. (2.9) that involve the loop function $A(q_2)$, it is more convenient to proceed in a different way to avoid a complicated angular integration:

$$\begin{aligned} &V_{2\pi}(\vec{r}_{12},\vec{r}_{32}) \\ &= \int \frac{d^3q_1}{(2\pi)^3}\frac{d^3q_2}{(2\pi)^3}\frac{d^3q_3}{(2\pi)^3}(2\pi)^3\delta^3(\vec{q}_1+\vec{q}_2+\vec{q}_3)e^{i\vec{q}_1\cdot\vec{r}_1} \\ &\quad \times e^{i\vec{q}_2\cdot\vec{r}_2}\, e^{i\vec{q}_3\cdot\vec{r}_3}\, V_{2\pi}(\vec{q}_1,\vec{q}_2,\vec{q}_3) \\ &= \int d^3r_0 \int \frac{d^3q_1}{(2\pi)^3}\frac{d^3q_2}{(2\pi)^3}\frac{d^3q_3}{(2\pi)^3} e^{i\vec{q}_1\cdot\vec{r}_{10}}\, e^{i\vec{q}_2\cdot\vec{r}_{20}} \\ &\quad \times e^{i\vec{q}_3\cdot\vec{r}_{30}}\, V_{2\pi}(\vec{q}_1,\vec{q}_2,\vec{q}_3) \\ &= -\frac{g_A^4 M_\pi^7}{4096\pi^3 F_\pi^6}\vec{\sigma}_1\cdot\vec{\nabla}_{12}\, \vec{\sigma}_3\cdot\vec{\nabla}_{32}\big[\boldsymbol{\tau}_1\cdot\boldsymbol{\tau}_3\big(2-\nabla_{12}^2-\nabla_{32}^2 \\ &\quad - 2\vec{\nabla}_{12}\cdot\vec{\nabla}_{32}\big)\big(3-3\nabla_{12}^2-3\nabla_{32}^2-4\vec{\nabla}_{12}\cdot\vec{\nabla}_{32}\big) \\ &\quad + \boldsymbol{\tau}_1\times\boldsymbol{\tau}_3\cdot\boldsymbol{\tau}_2\, \vec{\nabla}_{12}\times\vec{\nabla}_{32}\cdot\vec{\sigma}_2\, \big(4-\nabla_{12}^2-\nabla_{32}^2 \\ &\quad - 2\vec{\nabla}_{12}\cdot\vec{\nabla}_{32}\big)\big]\frac{1}{4\pi}\int d^3x U_1(|\vec{x}_{12}+\vec{x}\,|)\, W_1(x) \\ &\quad \times U_1(|\vec{x}_{32}+\vec{x}\,|), \end{aligned} \tag{2.14}$$

where

$$W_1(x) = \frac{4\pi}{M_\pi^2}\int \frac{d^3q}{(2\pi)^3} e^{i\vec{q}\cdot\vec{x}/M_\pi} A(q) = \frac{e^{-2x}}{2x^2}. \tag{2.15}$$

For various techniques to evaluate the integral in the last line of Eq. (2.14) the reader is referred to Ref. [15].

B. Two-pion-one-pion exchange topology

Consider now the 2π-1π 3NF arising from diagrams shown in Fig. 3 corresponding to topology (b) in Fig. 1. They can be written in the form

$$\begin{aligned} &V_{2\pi\text{-}1\pi} \\ &= \frac{\vec{\sigma}_3\cdot\vec{q}_3}{q_3^2+M_\pi^2}[\boldsymbol{\tau}_1\cdot\boldsymbol{\tau}_3\, (\vec{\sigma}_2\cdot\vec{q}_1\, \vec{q}_1\cdot\vec{q}_3\, F_1(q_1) \\ &\quad + \vec{\sigma}_2\cdot\vec{q}_1\, F_2(q_1) + \vec{\sigma}_2\cdot\vec{q}_3\, F_3(q_1)) \\ &\quad + \boldsymbol{\tau}_2\cdot\boldsymbol{\tau}_3\, (\vec{\sigma}_1\cdot\vec{q}_1\, \vec{q}_1\cdot\vec{q}_3\, F_4(q_1) \\ &\quad + \vec{\sigma}_1\cdot\vec{q}_3\, F_5(q_1) + \vec{\sigma}_2\cdot\vec{q}_1\, F_6(q_1) + \vec{\sigma}_2\cdot\vec{q}_3\, F_7(q_1)) \\ &\quad + \boldsymbol{\tau}_1\times\boldsymbol{\tau}_2\cdot\boldsymbol{\tau}_3\, \vec{\sigma}_1\times\vec{\sigma}_2\cdot\vec{q}_1\, F_8(q_1)], \end{aligned} \tag{2.16}$$

with $F_{1,\ldots,8}(q_1)$ being scalar functions. Using the formal expressions for the effective Hamiltonian from Ref. [24] we obtain the following result for the first six graphs:

$$\begin{aligned} F_1(q_1) &= -\frac{g_A^6}{256\pi F_\pi^6}\left[\frac{M_\pi}{4M_\pi^2+q_1^2} + \frac{2M_\pi}{q_1^2} \right. \\ &\quad \left. - \frac{8M_\pi^2+q_1^2}{q_1^2}A(q_1)\right], \\ F_3(q_1) &= -\frac{g_A^6}{256\pi F_\pi^6}\left[3M_\pi + \left(8M_\pi^2+3q_1^2\right)A(q_1)\right], \\ F_4(q_1) &= -\frac{1}{q_1^2}F_5(q_1) = -\frac{g_A^6}{128\pi F_\pi^6}\, A(q_1). \end{aligned} \tag{2.17}$$

Consider now diagrams (7)–(15), which involve one insertion of the Weinberg-Tomozawa vertex. The first three graphs only

contribute to the functions $F_{1,3}(q_1)$:

$$F_1(q_1) = \frac{g_A^4}{256\pi F_\pi^6}\left[\frac{M_\pi}{q_1^2} + \frac{q_1^2 - 4M_\pi^2}{q_1^2}A(q_1)\right],$$
$$F_3(q_1) = \frac{g_A^4}{256\pi F_\pi^6}\left[M_\pi + \left(q_1^2 + 4M_\pi^2\right)A(q_1)\right]. \quad (2.18)$$

We find that diagrams (10) and (11) do not generate a 3NF whereas the contribution from graphs (12)–(15) has the form

$$F_2(q_1) = \frac{g_A^4}{128\pi F_\pi^6}\left[M_\pi + \left(q_1^2 + 2M_\pi^2\right)A(q_1)\right]. \quad (2.19)$$

The next two diagrams (16) and (17) do not involve reducible topologies and can be dealt with by using the Feynman graph technique. It is easy to see that their contribution to the scattering amplitude is suppressed by $1/m$ owing to the time derivative that enters the Weinberg-Tomozawa vertices. The next two diagrams (18) and (19) yield vanishing contributions to the 3NF for exactly the same reason as do the two-pion exchange diagrams $\propto g_A^4$ at order $\nu = 2$. Next, the contribution from diagram (20) reads

$$F_6(q_1) = 2F_7(q_1) = \frac{g_A^4}{64\pi F_\pi^6}\left[M_\pi + \left(q_1^2 + 2M_\pi^2\right)A(q_1)\right],$$
$$F_8(q_1) = -\frac{g_A^4}{512\pi F_\pi^6}\left[M_\pi + \left(q_1^2 + 4M_\pi^2\right)A(q_1)\right]. \quad (2.20)$$

Here, we again use the choice $\alpha = 0$. Finally, it is easy to see that the last Feynman diagram (21) in Fig. 3 yields a vanishing result at the order considered.

The coordinate-space representation of the 2π-1π 3NF can be obtained straightforwardly by employing the same Fourier-type integrations as in the the first line of Eq. (2.14). This leads to the following expression where short-range terms resulting from constant contributions to $F_{2,3,6,7,8}$, which are proportional to M_π, are not shown:

$$\begin{aligned}
&V_{2\pi\text{-}1\pi}(\vec{r}_{12}, \vec{r}_{32}) \\
&= \frac{g_A^4 M_\pi^7}{8192\pi^3 F_\pi^6}\vec{\sigma}_3 \cdot \vec{\nabla}_{32}\,(2\boldsymbol{\tau}_1 \cdot \boldsymbol{\tau}_3 \\
&\quad \times \big[\vec{\sigma}_2 \cdot \vec{\nabla}_{12}\,\vec{\nabla}_{12} \cdot \vec{\nabla}_{32}\big(-2g_A^2 U_1(2x_{12}) \\
&\quad + \left(1 + g_A^2\right)W_1(x_{12}) + \left(1 - 2g_A^2\right)W_3(x_{12})\big) \\
&\quad - 2\vec{\sigma}_2 \cdot \vec{\nabla}_{12}(2W_1(x_{12}) + W_2(x_{12})\big) \\
&\quad - \vec{\sigma}_2 \cdot \vec{\nabla}_{32}\big(4\left(1 - 2g_A^2\right)W_1(x_{12}) + \left(1 - 3g_A^2\right)W_2(x_{12})\big)\big] \\
&\quad - 4\boldsymbol{\tau}_2 \cdot \boldsymbol{\tau}_3\big[g_A^2\,\vec{\sigma}_1 \cdot \vec{\nabla}_{12}\,\vec{\nabla}_{12} \cdot \vec{\nabla}_{32}\,W_1(x_{12}) \\
&\quad + g_A^2\,\vec{\sigma}_1 \cdot \vec{\nabla}_{32}\,W_2(x_{12}) + 2\,\vec{\sigma}_2 \cdot \vec{\nabla}_{12}\,(2W_1(x_{12}) \\
&\quad + W_2(x_{12})) + \vec{\sigma}_2 \cdot \vec{\nabla}_{32}\,(2W_1(x_{12}) + W_2(x_{12}))\big] \\
&\quad + \boldsymbol{\tau}_1 \times \boldsymbol{\tau}_2 \cdot \boldsymbol{\tau}_3\,\vec{\sigma}_1 \times \vec{\sigma}_2 \cdot \vec{\nabla}_{12}(4W_1(x_{12}) \\
&\quad + W_2(x_{12}))\big)U_1(x_{32}),
\end{aligned} \quad (2.21)$$

with

$$W_2(x) = -\nabla_x^2 W_1(x) = -\frac{e^{-2x}}{x^4}[1 + 2x(1 + x)],$$
$$\begin{aligned}
W_3(x) &= \frac{4\pi}{M_\pi^2}\int \frac{d^3q}{(2\pi)^3}\,e^{i\vec{q}\cdot\vec{x}/M_\pi}\left[\frac{M_\pi}{q^2} - \frac{4M_\pi^2}{q^2}A(q)\right] \\
&= 2Ei(-2x) + \frac{e^{-2x}}{x},
\end{aligned} \quad (2.22)$$

and

$$Ei(x) \equiv -\int_{-x}^{\infty}\frac{e^{-t}dt}{t}. \quad (2.23)$$

We emphasize again that these expressions are only valid at large distances.

C. Ring diagrams

We now regard ring diagrams shown in Fig. 4, which correspond to topology (c) in Fig. 1. These are most cumbersome to evaluate. The contributions from the first two diagrams can be obtained by using the expressions for the effective Hamilton operator given in Ref. [24]. This leads to the following structures:

$$V_{\text{ring}}^1 = M^1\left[\frac{4}{\omega_a^3\omega_b\omega_c} + \frac{4}{\omega_a\omega_b^3\omega_c} - \frac{4}{\omega_a\omega_b\,\omega_c^3}\right],$$
$$V_{\text{ring}}^2 = M^2\left[-\frac{4}{\omega_a^3\omega_b\omega_c} - \frac{4}{\omega_a\omega_b^3\omega_c} - \frac{4}{\omega_a\omega_b\,\omega_c^3}\right], \quad (2.24)$$

where M^i represents the spin, isospin, and momentum structure that results from the vertices entering the diagram i and ω denotes the pion free energy, $\omega \equiv \sqrt{q^2 + M_\pi^2}$. By substituting the expressions for the vertices, the result can be written in the form

$$\begin{aligned}
V_{\text{ring}} &= \left(\frac{g_A}{2F_\pi}\right)^6 \frac{1}{(2\pi)^3}\int d^3l_1 d^3l_2 d^3l_3 \delta^3(\vec{l}_3 - \vec{l}_2 - \vec{q}_1) \\
&\quad \times \delta^3(\vec{l}_2 - \vec{l}_1 - \vec{q}_3)\frac{v}{\left[l_1^2 + M_\pi^2\right]\left[l_2^2 + M_\pi^2\right]^2\left[l_3^2 + M_\pi^2\right]},
\end{aligned} \quad (2.25)$$

with the numerator

$$\begin{aligned}
v &= -8\boldsymbol{\tau}_1 \cdot \boldsymbol{\tau}_2\,\vec{l}_1 \times \vec{l}_3 \cdot \vec{\sigma}_2\,\vec{l}_1 \times \vec{l}_2 \cdot \vec{\sigma}_3\,\vec{l}_2 \cdot \vec{l}_3 \\
&\quad - 4\boldsymbol{\tau}_1 \cdot \boldsymbol{\tau}_3\,\vec{l}_1 \cdot \vec{l}_2\,\vec{l}_1 \cdot \vec{l}_3\,\vec{l}_2 \cdot \vec{l}_3 + 2\boldsymbol{\tau}_1 \times \boldsymbol{\tau}_2 \cdot \boldsymbol{\tau}_3\,\vec{l}_1 \\
&\quad \times \vec{l}_3 \cdot \vec{\sigma}_2\vec{l}_1 \cdot \vec{l}_2\,\vec{l}_2 \cdot \vec{l}_3 + 6\vec{l}_2 \times \vec{l}_3 \cdot \vec{\sigma}_1\,\vec{l}_1 \times \vec{l}_2 \cdot \vec{\sigma}_3\,\vec{l}_1 \cdot \vec{l}_3.
\end{aligned} \quad (2.26)$$

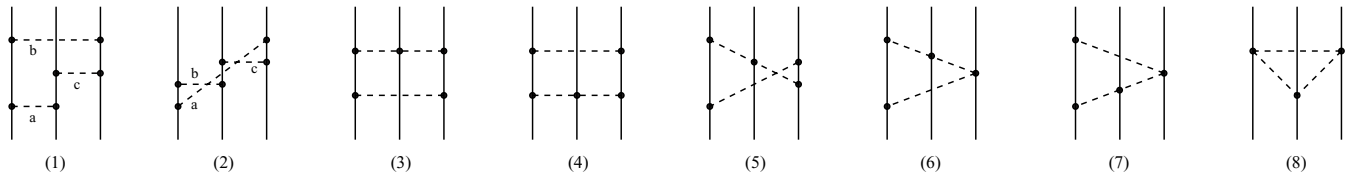

FIG. 4. Ring diagrams at N^{3}LO. Graphs resulting from the interchange of the nucleon lines are not shown. For notation see Figs. 1 and 2.

Carrying out the two trivial integrations over, say, l_1 and l_2 leads to the standard three-point function integrals. The latter can be evaluated but the resulting expressions are rather involved (see the Appendix). It is more convenient to evaluate Eq. (2.25) in configuration space by using again the same definition as in the the first line of Eq. (2.11). This leads to the following compact result:

$$
\begin{aligned}
&V_{\rm ring}(\vec r_{12},\vec r_{32}) \\
&= \left(\frac{g_A}{2F_\pi}\right)^6 \int \frac{d^3l_1}{(2\pi)^3}\frac{d^3l_2}{(2\pi)^3}\frac{d^3l_3}{(2\pi)^3}\, e^{i\vec l_1\cdot\vec r_{23}}\, e^{i\vec l_2\cdot\vec r_{31}}\, e^{i\vec l_3\cdot\vec r_{12}} \\
&\quad\times \frac{v}{\left[l_1^2+M_\pi^2\right]\left[l_2^2+M_\pi^2\right]^2\left[l_3^2+M_\pi^2\right]} \\
&= -\frac{g_A^6 M_\pi^7}{4096\pi^3 F_\pi^6} \\
&\quad\times[-4\boldsymbol{\tau}_1\cdot\boldsymbol{\tau}_2\,\vec\nabla_{23}\times\vec\nabla_{12}\cdot\vec\sigma_2\,\vec\nabla_{23}\times\vec\nabla_{31}\cdot\vec\sigma_3\,\vec\nabla_{31}\cdot\vec\nabla_{12} \\
&\quad-2\boldsymbol{\tau}_1\cdot\boldsymbol{\tau}_3\,\vec\nabla_{23}\cdot\vec\nabla_{31}\,\vec\nabla_{23}\cdot\vec\nabla_{12}\,\vec\nabla_{31}\cdot\vec\nabla_{12} \\
&\quad+\boldsymbol{\tau}_1\times\boldsymbol{\tau}_2\cdot\boldsymbol{\tau}_3\,\vec\nabla_{23}\times\vec\nabla_{12}\cdot\vec\sigma_2\,\vec\nabla_{23}\cdot\vec\nabla_{31}\,\vec\nabla_{31}\cdot\vec\nabla_{12} \\
&\quad+3\vec\nabla_{31}\times\vec\nabla_{12}\cdot\vec\sigma_1\,\vec\nabla_{23}\times\,\vec\nabla_{31}\cdot\vec\sigma_3\,\vec\nabla_{23}\cdot\vec\nabla_{12}] \\
&\quad\times U_1(x_{23})\,U_2(x_{31})\,U_1(x_{12}),
\end{aligned}
\tag{2.27}
$$

where the derivatives should be evaluated as if the variables $\vec x_{12}$, $\vec x_{23}$, and $\vec x_{31}$ were independent[4] and we have introduced

$$
U_2(x) = 8\pi M_\pi \int \frac{d^3q}{(2\pi)^3}\frac{e^{i\vec q\cdot\vec x/M_\pi}}{\left[q^2+M_\pi^2\right]^2} = e^{-x}. \tag{2.28}
$$

Consider now diagrams (3)–(5) in Fig. 3, which involve one insertion of the Weinberg-Tomozawa vertex. The corresponding contribution to the 3NF can be evaluated in a similar way as previously described and by using the explicit expressions for the effective Hamilton operator from Ref. [24]. We find that graphs (3) and (4) lead to vanishing 3NF whereas the contribution from diagram (5) reads

$$
\begin{aligned}
&V_{\rm ring}(\vec r_{12},\vec r_{32}) \\
&= \frac{g_A^4 M_\pi^7}{2048\pi^3 F_\pi^6}[2\boldsymbol{\tau}_1\cdot\boldsymbol{\tau}_2\,(\vec\nabla_{23}\cdot\vec\nabla_{31}\,\vec\nabla_{31}\cdot\vec\nabla_{12} \\
&\quad-\vec\nabla_{31}\times\vec\nabla_{12}\cdot\vec\sigma_1\,\vec\nabla_{23}\times\vec\nabla_{31}\cdot\vec\sigma_3) \\
&\quad+\boldsymbol{\tau}_1\times\boldsymbol{\tau}_2\cdot\boldsymbol{\tau}_3\,\vec\nabla_{31}\times\vec\nabla_{12}\cdot\vec\sigma_1\,\vec\nabla_{23}\cdot\vec\nabla_{31}] \\
&\quad\times U_1(x_{23})\,U_1(x_{31})\,U_1(x_{12}).
\end{aligned}
\tag{2.29}
$$

Finally, we found that the contributions from the last three diagrams in Fig. 3 are suppressed by the factor $1/m$ and, therefore, need not to be taken into account at the order considered.

III. SUMMARY AND CONCLUSIONS

In this work, we have derived the long-range contributions of the 3NF in chiral effective field theory at N^{3}LO in the chiral expansion. These results constitute the first systematic corrections to the leading 2π exchange that appears at N^{2}LO in the Weinberg counting. We have shown that there exists three different topologies that contribute to the long-range components of the chiral 3NF. Although some of these simply renormalize the LECs of the leading order 2π exchange topology, there are many new spin-isospin structures generated at N^{3}LO from all three topologies. We have given the momentum- and coordinate-space representations of the various contributions. At this order, there is an arbitrariness in choosing the multipion interactions [cf. Eq. (2.2)] that allows us to shuffle strength among the various contributions. The individual contributions presented in this work are given for the specific choice $\alpha = 0$. We have explicitly verified that the sum of all diagrams contributing to the 3NF is independent of the choice of this parameter as demanded by field theory. It is important to stress that the corrections to the 3NF discussed here are local and free of any unknown low-energy constants and can be expressed entirely in terms of the nucleon axial-vector coupling g_A, the pion decay constant F_π, and the pion mass M_π. It should further be emphasized that the dimension-two LECs c_3 and c_4 that enter the leading 3NF and would also contribute at N^{4}LO are larger than their natural values $c_i \sim g_A/(4\pi F_\pi) \sim 1$ GeV^{-1} [21]. This is understood in terms of $\Delta(1232)$, s-channel and vector-meson t-channel excitations [25]. It is, therefore, expected that the theory with explicit spin-3/2 degrees of freedom leads to an improved convergence as compared to the pure pion-nucleon theory considered here. Of course, the theory with explicit deltas leads to many more structures and has also been much less developed phenomenologically. Still, it is important to confront the results obtained here with similarly accurate calculations in the delta-full theory. Work along these lines is in progress.

ACKNOWLEDGMENTS

The work of E. E. and H. K. was supported in part by funds provided from the Helmholtz Association to the young investigator group "Few-Nucleon Systems in Chiral Effective Field Theory" (Grant No. VH-NG-222) and through the virtual institute "Spin and Strong QCD" (Grant No. VH-VI-231). This work was further supported by the DFG (SFB/TR 16 "Subnuclear Structure of Matter") and by the EU Integrated Infrastructure Initiative Hadron Physics Project under Contract No. RII3-CT-2004-506078.

APPENDIX: EXPRESSIONS FOR RING DIAGRAMS IN MOMENTUM SPACE

In this appendix we give lengthy expressions for the ring diagrams in Fig. 4 in momentum space. The contributions from diagrams (1) and (2) can be expressed as

$$
\begin{aligned}
V_{\rm ring} &= \vec\sigma_1\cdot\vec\sigma_2\;\boldsymbol{\tau}_2\cdot\boldsymbol{\tau}_3\;R_1 + \vec\sigma_1\cdot\vec q_1\vec\sigma_2\cdot\vec q_1\;\boldsymbol{\tau}_2\cdot\boldsymbol{\tau}_3\;R_2 \\
&\quad+\vec\sigma_1\cdot\vec q_1\vec\sigma_2\cdot\vec q_3\;\boldsymbol{\tau}_2\cdot\boldsymbol{\tau}_3\;R_3 + \vec\sigma_1\cdot\vec q_3\vec\sigma_2\cdot\vec q_1\;\boldsymbol{\tau}_2\cdot\boldsymbol{\tau}_3\;R_4 \\
&\quad+\vec\sigma_1\cdot\vec q_3\vec\sigma_2\cdot\vec q_3\;\boldsymbol{\tau}_2\cdot\boldsymbol{\tau}_3\;R_5 + \boldsymbol{\tau}_1\cdot\boldsymbol{\tau}_3\;R_6 \\
&\quad+\vec\sigma_1\cdot\vec q_1\vec\sigma_3\cdot\vec q_1\;R_7 + \vec\sigma_1\cdot\vec q_1\vec\sigma_3\cdot\vec q_3\;R_8
\end{aligned}
$$

[4] Clearly, the relative distances $\vec r_{12}$, $\vec r_{23}$, and $\vec r_{31}$ are related via $\vec r_{12}+\vec r_{23}+\vec r_{31}=0$.

$$+\vec{\sigma}_1\cdot\vec{q}_3\vec{\sigma}_3\cdot\vec{q}_1\ R_9+\vec{\sigma}_1\cdot\vec{\sigma}_3\ R_{10}$$
$$+\vec{q}_1\cdot\vec{q}_3\times\vec{\sigma}_2\ \boldsymbol{\tau}_1\cdot\boldsymbol{\tau}_2\times\boldsymbol{\tau}_3\ R_{11}, \tag{A1}$$

where the functions $R_i \equiv R_i(q_1, q_3, z)$ with $z = \hat{q}_1\cdot\hat{q}_3$ are defined as follows:

$$\begin{aligned}
R_1 &= \frac{(-1+z^2)g_A^6M_\pi\big(2M_\pi^2+q_3^2\big)\big(q_2^2q_3+4M_\pi^2(zq_1+q_3)\big)}{128F^6\pi\big(4(-1+z^2)M_\pi^2-q_2^2\big)\big(4M_\pi^2q_3+q_3^3\big)}-\frac{A(q_2)g_A^6q_2^2\big(2M_\pi^2(q_1+zq_3)+zq_3\big(-q_1^2+q_3^2\big)\big)}{128F^6\pi(-1+z^2)q_1q_3^2}\\
&-\frac{A(q_3)g_A^6\big(zq_2^2(zq_1-q_3)q_3+2M_\pi^2\big(z(-2+z^2)q_1^2-(1+z^2)q_1q_3-zq_3^2\big)\big)}{128F^6\pi(-1+z^2)q_1q_3}\\
&+\frac{A(q_1)g_A^6\big(2M_\pi^2q_2^2+q_3\big(-zq_1^3+(2-3z^2)q_1^2q_3-z(-2+z^2)q_1q_3^2+q_3^3\big)\big)}{128F^6\pi(-1+z^2)q_3^2}\\
&-\frac{I(4:0,-q_1,q_3;0)g_A^6q_2^2}{32F^6(-1+z^2)\big(4(-1+z^2)M_\pi^2-q_2^2\big)q_3}\big(8(-1+z^2)M_\pi^4(2zq_1+(1+z^2)q_3)\\
&+q_2^2q_3\big(z^2q_1^2+z(-1+z^2)q_1q_3-q_3^2\big)+2M_\pi^2\big(z(-2+z^2)q_1^3-(1+2z^2)q_1^2q_3+3z(-2+z^2)q_1q_3^2+(-3+2z^4)q_3^3\big)\big),\\
R_2 &= \frac{A(q_2)g_A^6q_2^2\big(-2M_\pi^2((1+z^2)q_1+2zq_3)+zq_3\big((1+z^2)q_1^2-2q_3^2\big)\big)}{128F^6\pi(-1+z^2)^2q_1^3q_3^2}\\
&+\frac{A(q_3)g_A^6\big(M_\pi^2\big(2zq_1^2+(1+3z^2)q_1q_3+2zq_3^2\big)+zq_3\big(-zq_1^3-z^2q_1^2q_3+zq_1q_3^2+q_3^3\big)\big)}{64F^6\pi(-1+z^2)^2q_1^3q_3}\\
&+\frac{A(q_1)g_A^6}{128F^6\pi(-1+z^2)^2q_1^2q_3^2}\big(2M_\pi^2((1+z^2)q_1^2+z(3+z^2)q_1q_3+(1+z^2)q_3^2\big)\\
&+q_3\big(-(z+z^3)q_1^3+(2-5z^2+z^4)q_1^2q_3+z(1+z^2)q_1q_3^2+(1+z^2)q_3^3\big)\big)\\
&-\frac{I(4:0,-q_1,q_3;0)g_A^6}{32F^6(-1+z^2)^2q_1^2\big(-4(-1+z^2)M_\pi^2+q_2^2\big)q_3}\big(q_2^4q_3\big(-2z^2q_1^2+(1+z^2)q_3^2\big)\\
&-8(-1+z)(1+z)M_\pi^4\big(z(2+z^2)q_1^3+(1+2z^2)^2q_1^2q_3+z(2+7z^2)q_1q_3^2+(1+2z^2)q_3^3\big)\\
&+2M_\pi^2q_2^2\big(2zq_1^3+(1-z^2+6z^4)q_1^2q_3-2z(-1-3z^2+z^4)q_1q_3^2+(3+3z^2-4z^4)q_3^3\big)\big)\\
&+\frac{g_A^6M_\pi\big(2M_\pi^2+q_3^2\big)\big(q_2^2q_3+4M_\pi^2(zq_1+q_3)\big)}{128F^6\pi q_1^2\big(4(-1+z^2)M_\pi^2-q_2^2\big)\big(4M_\pi^2q_3+q_3^3\big)},\\
R_3 &= -\frac{zA(q_2)g_A^6q_2^2\big(-4M_\pi^2(q_1+zq_3)+q_3\big(2zq_1^2+(-1+z^2)q_1q_3-2zq_3^2\big)\big)}{128F^6\pi(-1+z^2)^2q_1^2q_3^3}\\
&-\frac{zA(q_3)g_A^6}{128F^6\pi(-1+z^2)^2q_1^2q_3^2}\big(M_\pi^2\big(-2z(-3+z^2)q_1^2+4(1+z^2)q_1q_3+4zq_3^2\big)+q_3\big(-(1+z^2)q_1^3\\
&-2z^3q_1^2q_3+(1+z^2)q_1q_3^2+2zq_3^3\big)\big)\\
&-\frac{zA(q_1)g_A^6\big(2M_\pi^2\big(2q_1^2+4zq_1q_3+(1+z^2)q_3^2\big)+q_3\big(-2zq_1^3+(1-3z^2)q_1^2q_3+2zq_1q_3^2+(1+z^2)q_3^3\big)\big)}{128F^6\pi(-1+z^2)^2q_1q_3^3}\\
&-\frac{I(4:0,-q_1,q_3;0)zg_A^6}{32F^6(-1+z^2)^2q_1\big(-4(-1+z^2)M_\pi^2+q_2^2\big)q_3^2}\big(q_2^4q_3\big((1+z^2)q_1^2+z(-1+z^2)q_1q_3-(1+z^2)q_3^2\big)\\
&+8(-1+z)(1+z)M_\pi^4\big(3zq_1^3+(-1+10z^2)q_1^2q_3+3z(1+2z^2)q_1q_3^2+(1+2z^2)q_3^3\big)\\
&+2M_\pi^2q_2^2\big(z(-3+z^2)q_1^3+(3-9z^2)q_1^2q_3-z(5+z^2)q_1q_3^2+(-3-3z^2+4z^4)q_3^3\big)\big)\\
&+\frac{zg_A^6M_\pi\big(2M_\pi^2+q_3^2\big)\big(q_2^2q_3+4M_\pi^2(zq_1+q_3)\big)}{128F^6\pi q_1\big(-4(-1+z^2)M_\pi^2+q_2^2\big)q_3^2\big(4M_\pi^2+q_3^2\big)},
\end{aligned}$$

$$
\begin{aligned}
R_4 &= \frac{A(q_2)g_A^6 q_2^2\big(-2z^2q_1^2q_3+(1+z^2)q_3^3+2M_\pi^2\big(2zq_1+(1+z^2)q_3\big)\big)}{128F^6\pi(-1+z^2)^2q_1^2q_3^3}\\
&+\frac{A(q_1)g_A^6\big(-2M_\pi^2\big(2zq_1^2+(1+3z^2)q_1q_3+2zq_3^2\big)+q_3\big(2z^2q_1^3+2z^3q_1^2q_3+(1-4z^2+z^4)q_1q_3^2-2zq_3^3\big)\big)}{128F^6\pi(-1+z^2)^2q_1q_3^3}\\
&-\frac{A(q_3)g_A^6}{128F^6\pi(-1+z^2)^2q_1^2q_3^2}\big(2M_\pi^2\big(-z^2(-3+z^2)q_1^2+z(3+z^2)q_1q_3+(1+z^2)q_3^2\big)\\
&+q_3\big(-(z+z^3)q_1^3-(1-z^2+2z^4)q_1^2q_3+z(1+z^2)q_1q_3^2+(1+z^2)q_3^3\big)\big)\\
&-\frac{I(4:0,-q_1,q_3;0)g_A^6}{32F^6(-1+z^2)^2q_1\big(-4(-1+z^2)M_\pi^2+q_2^2\big)q_3^2}\big(q_2^4q_3\big((z+z^3)q_1^2+(-1+z^2)^2q_1q_3-2zq_3^2\big)\\
&+8(-1+z)(1+z)M_\pi^4\big(3z^2q_1^3+9z^3q_1^2q_3+(-2+9z^2+2z^4)q_1q_3^2+z(2+z^2)q_3^3\big)\\
&+2M_\pi^2q_2^2\big(z^2(-3+z^2)q_1^3+(2z-8z^3)q_1^2q_3+(4+5z^2(-3+z^2))q_1q_3^2+2z(-3+z^2+z^4)q_3^3\big)\big)\\
&+\frac{zg_A^6M_\pi\big(2M_\pi^2+q_3^2\big)\big(q_2^2q_3+4M_\pi^2(zq_1+q_3)\big)}{128F^6\pi q_1\big(-4(-1+z^2)M_\pi^2+q_2^2\big)q_3^2\big(4M_\pi^2+q_3^2\big)},\\
R_5 &= \frac{A(q_2)g_A^6q_2^2\big(-4M_\pi^2(q_1+zq_3)+q_3\big(2zq_1^2+(-1+z^2)q_1q_3-2zq_3^2\big)\big)}{128F^6\pi(-1+z^2)^2q_1q_3^4}\\
&-\frac{A(q_3)g_A^6}{128F^6\pi(-1+z^2)^2q_1q_3^3}\big(2M_\pi^2\big(z(-3+z^2)q_1^2-2(1+z^2)q_1q_3-2zq_3^2\big)+q_3\big((1+z^2)q_1^3+2z^3q_1^2q_3-(1+z^2)q_1q_3^2\\
&-2zq_3^3\big)\big)+\frac{A(q_1)g_A^6\big(2M_\pi^2\big(2q_1^2+4zq_1q_3+(1+z^2)q_3^2\big)+q_3\big(-2zq_1^3+(1-3z^2)q_1^2q_3+2zq_1q_3^2+(1+z^2)q_3^3\big)\big)}{128F^6\pi(-1+z^2)^2q_3^4}\\
&+\frac{I(4:0,-q_1,q_3;0)g_A^6}{32F^6(-1+z^2)^2\big(-4(-1+z^2)M_\pi^2+q_2^2\big)q_3^3}\big(q_2^4q_3((1+z^2)q_1^2+z(-1+z^2)q_1q_3-(1+z^2)q_3^2\big)\\
&+8(-1+z)(1+z)M_\pi^4\big(3zq_1^3+(-1+10z^2)q_1^2q_3+3z(1+2z^2)q_1q_3^2+(1+2z^2)q_3^3\big)\\
&+2M_\pi^2q_2^2(z(-3+z^2)q_1^3+(3-9z^2)q_1^2q_3-z(5+z^2)q_1q_3^2+(-3-3z^2+4z^4)q_3^3\big)\big)\\
&-\frac{g_A^6M_\pi\big(2M_\pi^2+q_3^2\big)\big(q_2^2q_3+4M_\pi^2(zq_1+q_3)\big)}{128F^6\pi\big(-4(-1+z^2)M_\pi^2+q_2^2\big)q_3^3\big(4M_\pi^2+q_3^2\big)},\\
R_6 &= \frac{A(q_2)g_A^6\big(2M_\pi^2+q_2^2\big)}{128F^6\pi}+\frac{A(q_1)g_A^6\big(2z\big(M_\pi^2+q_1^2\big)q_3+q_1\big(8M_\pi^2+3q_1^2+q_3^2\big)\big)}{128F^6\pi q_1}\\
&+\frac{A(q_3)g_A^6\big(2zq_1\big(M_\pi^2+q_3^2\big)+q_3\big(8M_\pi^2+q_1^2+3q_3^2\big)\big)}{128F^6\pi q_3}\\
&-\frac{g_A^6M_\pi}{128F^6\pi q_1\big(4M_\pi^2+q_1^2\big)\big(4(-1+z^2)M_\pi^2-q_2^2\big)q_3\big(4M_\pi^2+q_3^2\big)}\big((5+z^2)q_1^3q_2^2q_3^3+8M_\pi^6\big(z(-3+4z^2)q_1^2\\
&+2(19-18z^2)q_1q_3+z(-3+4z^2)q_3^2\big)+2M_\pi^4\big(4z(-1+z^2)q_1^4+(77-36z^2)q_1^3q_3+2z(33+8z^2)q_1^2q_3^2\\
&+(77-36z^2)q_1q_3^3+4z(-1+z^2)q_3^4\big)+2M_\pi^2q_1q_3\big((10+z^2)q_1^4+2z(9+2z^2)q_1^3q_3+(29-7z^2)q_1^2q_3^2\\
&+2z(9+2z^2)q_1q_3^3+(10+z^2)q_3^4\big)\big)-\frac{I(4:0,-q_1,q_3;0)g_A^6\big(2M_\pi^2+q_2^2\big)}{32F^6q_1\big(-4(-1+z^2)M_\pi^2+q_2^2\big)q_3}\big(q_1q_2^2q_3\big(q_1^2+zq_1q_3+q_3^2\big)\\
&+4M_\pi^4\big(zq_1^2-2(-2+z^2)q_1q_3+zq_3^2\big)+2M_\pi^2\big(4q_1q_3\big(q_1^2+q_3^2\big)+z\big(q_1^4+6q_1^2q_3^2+q_3^4\big)\big)\big),\\
R_7 &= \frac{3g_A^6M_\pi\big(2M_\pi^2+q_2^2\big)}{256F^6\pi q_1^2\big(-4(-1+z^2)M_\pi^2+q_2^2\big)}-\frac{3A(q_3)g_A^6\big(2M_\pi^2+q_2^2\big)((1+z^2)q_1+2zq_3)}{256F^6\pi(-1+z^2)^2q_1^3}\\
&-\frac{3A(q_1)g_A^6\big(2M_\pi^2+q_2^2\big)(2zq_1+(1+z^2)q_3)}{256F^6\pi(-1+z^2)^2q_1^2q_3}+\frac{3A(q_2)g_A^6\big(2M_\pi^2+q_2^2\big)\big(2zq_1^2+(1+3z^2)q_1q_3+2zq_3^2\big)}{256F^6\pi(-1+z^2)^2q_1^3q_3}
\end{aligned}
$$

$$
\begin{aligned}
&+\frac{3I(4:0,-q_1,q_3;0)g_A^6\left(2M_\pi^2+q_2^2\right)}{64F^6(-1+z^2)^2q_1^2\left(4(-1+z^2)M_\pi^2-q_2^2\right)}\Big(-q_2^2\big((1+z^2)q_1^2+z(3+z^2)q_1q_3+(1+z^2)q_3^2\big)\\
&+4(-1+z^2)M_\pi^2\big((1+2z^2)q_1^2+2z(2+z^2)q_1q_3+(1+2z^2)q_3^2\big)\Big),\\
R_8=&-\frac{3zg_A^6M_\pi\left(2M_\pi^2+q_2^2\right)}{256F^6\pi q_1\left(-4(-1+z^2)M_\pi^2+q_2^2\right)q_3}+\frac{3zA(q_3)g_A^6\left(2M_\pi^2+q_2^2\right)\big((1+z^2)q_1+2zq_3\big)}{256F^6\pi(-1+z^2)^2q_1^2q_3}\\
&+\frac{3zA(q_1)g_A^6\left(2M_\pi^2+q_2^2\right)(2zq_1+(1+z^2)q_3)}{256F^6\pi(-1+z^2)^2q_1q_3^2}-\frac{3zA(q_2)g_A^6\left(2M_\pi^2+q_2^2\right)\big(2zq_1^2+(1+3z^2)q_1q_3+2zq_3^2\big)}{256F^6\pi(-1+z^2)^2q_1^2q_3^2}\\
&-\frac{3I(4:0,-q_1,q_3;0)zg_A^6\left(2M_\pi^2+q_2^2\right)}{64F^6(-1+z^2)^2q_1\left(4(-1+z^2)M_\pi^2-q_2^2\right)q_3}\Big(-q_2^2\big((1+z^2)q_1^2+z(3+z^2)q_1q_3+(1+z^2)q_3^2\big)\\
&+4(-1+z^2)M_\pi^2\big((1+2z^2)q_1^2+2z(2+z^2)q_1q_3+(1+2z^2)q_3^2\big)\Big),\\
R_9=&-\frac{3A(q_2)g_A^6\left(2M_\pi^2+q_2^2\right)\big((1+z^2)q_1^2+z(3+z^2)q_1q_3+(1+z^2)q_3^2\big)}{256F^6\pi(-1+z^2)^2q_1^2q_3^2}\\
&+\frac{3A(q_1)g_A^6\big((1+z^2)q_1^3+2z(2+z^2)q_1^2q_3-z^2(-7+z^2)q_1q_3^2+2zq_3^3+2M_\pi^2\big((1+z^2)q_1+2zq_3\big)\big)}{256F^6\pi(-1+z^2)^2q_1q_3^2}\\
&+\frac{3A(q_3)g_A^6\big(2zq_1^3-z^2(-7+z^2)q_1^2q_3+2z(2+z^2)q_1q_3^2+(1+z^2)q_3^3+2M_\pi^2(2zq_1+(1+z^2)q_3)\big)}{256F^6\pi(-1+z^2)^2q_1^2q_3}\\
&+\frac{3I(4:0,-q_1,q_3;0)zg_A^6\left(2M_\pi^2+q_2^2\right)}{64F^6(-1+z^2)^2q_1\left(-4(-1+z^2)M_\pi^2+q_2^2\right)q_3}\big(q_2^2\big(-2q_1^2+z(-5+z^2)q_1q_3-2q_3^2\big)\\
&+4(-1+z^2)M_\pi^2\big((2+z^2)q_1^2+6zq_1q_3+(2+z^2)q_3^2\big)\big)-\frac{3zg_A^6M_\pi\left(2M_\pi^2+q_2^2\right)}{256F^6\pi q_1\left(-4(-1+z^2)M_\pi^2+q_2^2\right)q_3},\\
R_{10}=&\frac{3(-1+z^2)g_A^6M_\pi\left(2M_\pi^2+q_2^2\right)}{256F^6\pi\left(-4(-1+z^2)M_\pi^2+q_2^2\right)}+\frac{3A(q_2)g_A^6\left(2M_\pi^2+q_2^2\right)(zq_1+q_3)(q_1+zq_3)}{256F^6\pi(-1+z^2)q_1q_3}\\
&-\frac{3A(q_1)g_A^6\big(zq_1^3+(1+2z^2)q_1^2q_3-z(-4+z^2)q_1q_3^2+q_3^3+2M_\pi^2(zq_1+q_3)\big)}{256F^6\pi(-1+z^2)q_3}\\
&-\frac{3A(q_3)g_A^6\big(q_1^3-z(-4+z^2)q_1^2q_3+(1+2z^2)q_1q_3^2+zq_3^3+2M_\pi^2(q_1+zq_3)\big)}{256F^6\pi(-1+z^2)q_1}\\
&+\frac{3I(4:0,-q_1,q_3;0)g_A^6\left(2M_\pi^2+q_2^2\right)}{64F^6(-1+z^2)\left(4(-1+z^2)M_\pi^2-q_2^2\right)}\Big(-q_2^2\big(q_1^2-z(-3+z^2)q_1q_3+q_3^2\big)\\
&+4(-1+z^2)M_\pi^2\big((1+z^2)q_1^2+4zq_1q_3+(1+z^2)q_3^2\big)\Big),\\
R_{11}=&-\frac{A(q_2)g_A^6q_2^2\left(4M_\pi^2+q_1^2+q_3^2\right)}{256F^6\pi(-1+z^2)q_1^2q_3^2}\\
&+\frac{A(q_3)g_A^6\big(2M_\pi^2\big((-1+z^2)q_1^2+2zq_1q_3+2q_3^2\big)+q_3\big(zq_1^3+(-1+2z^2)q_1^2q_3+zq_1q_3^2+q_3^3\big)\big)}{256F^6\pi(-1+z^2)q_1^2q_3^2}\\
&+\frac{A(q_1)g_A^6\big(2M_\pi^2\big(2q_1^2+2zq_1q_3+(-1+z^2)q_3^2\big)+q_1\big(q_1^3+zq_1^2q_3+(-1+2z^2)q_1q_3^2+zq_3^3\big)\big)}{256F^6\pi(-1+z^2)q_1^2q_3^2}\\
&-\frac{I(4:0,-q_1,q_3;0)g_A^6q_2^2}{\left(64F^6(-1+z^2)q_1^2\left(-4(-1+z^2)M_\pi^2+q_2^2\right)q_3^2\right)}\Big(-\left(2M_\pi^2+q_1^2\right)\left(2M_\pi^2+q_3^2\right)\left(4M_\pi^2+q_1^2+q_3^2\right)\\
&+2z^3q_1q_3\left(-4M_\pi^4+q_1^2q_3^2\right)+z^2\left(4M_\pi^2+q_1^2+q_3^2\right)\left(4M_\pi^4+3q_1^2q_3^2+2M_\pi^2\left(q_1^2+q_3^2\right)\right)\\
&+zq_1q_3\left(8M_\pi^4+q_1^4+q_3^4+4M_\pi^2\left(q_1^2+q_3^2\right)\right)\Big)
\end{aligned}
$$

$$-\frac{g_A^6 M_\pi}{256F^6\pi q_1^2\left(4M_\pi^2+q_1^2\right)\left(-4(-1+z^2)M_\pi^2+q_2^2\right)q_3^2\left(4M_\pi^2+q_3^2\right)}\Big(-2z^2\Big(4M_\pi^4q_1^2\left(4M_\pi^2+q_1^2\right)$$
$$+4M_\pi^2\left(2M_\pi^2+q_1^2\right)^2q_3^2+\left(2M_\pi^2+q_1^2\right)^2q_3^4\Big)+2M_\pi^2\left(4M_\pi^2+q_1^2+q_3^2\right)\left(q_1^2q_3^2+2M_\pi^2\left(q_1^2+q_3^2\right)\right)$$
$$-zq_1q_3\left(32M_\pi^6+12M_\pi^4\left(q_1^2+q_3^2\right)+q_1^2q_3^2\left(q_1^2+q_3^2\right)+2M_\pi^2\left(q_1^4+4q_1^2q_3^2+q_3^4\right)\right)\Big). \tag{A2}$$

In these expressions, q_1 and q_3 are always to be understood as the magnitudes of the corresponding three-momenta (except in the arguments of the function I) : $q_1 \equiv |\vec{q}_1|$ and $q_3 \equiv |\vec{q}_3|$. Further, the function $I(d : p_1, p_2, p_3; p_4)$ refers to the scalar loop integral

$$I(d : p_1, p_2, p_3; p_4)$$
$$= \frac{1}{i}\int\frac{d^dl}{(2\pi)^d}\frac{1}{(l+p_1)^2-M_\pi^2+i\epsilon}\frac{1}{(l+p_2)^2-M_\pi^2+i\epsilon}$$
$$\times\frac{1}{(l+p_3)^2-M_\pi^2+i\epsilon}\frac{1}{v\cdot(l+p_4)+i\epsilon}. \tag{A3}$$

In a general case, this function depends on the four-momenta p_i. For the case $p_i^0 = 0$ we are interested in, it can be expressed in terms of the three-point function in Euclidean space

$$J(d : \vec{p}_1, \vec{p}_2, \vec{p}_3) = \int\frac{d^dl}{(2\pi)^d}\frac{1}{(\vec{l}+\vec{p}_1)^2+M_\pi^2}\frac{1}{(\vec{l}+\vec{p}_2)^2+M_\pi^2}$$
$$\times\frac{1}{(\vec{l}+\vec{p}_3)^2+M_\pi^2}. \tag{A4}$$

In particular, the function $I(4 : 0, -q_1, q_3; 0)$ that enters the expressions for R_i can be written as

$$I(4 : 0, -q_1, q_3; 0) = \tfrac{1}{2}J(3 : \vec{0}, -\vec{q}_1, \vec{q}_3). \tag{A5}$$

For diagram (5), we obtain the following representation:

$$V_{\rm ring} = \boldsymbol{\tau}_1\cdot\boldsymbol{\tau}_2\ S_1+\vec{\sigma}_1\cdot\vec{q}_1\vec{\sigma}_3\cdot\vec{q}_1\ \boldsymbol{\tau}_1\cdot\boldsymbol{\tau}_2\ S_2$$
$$+\vec{\sigma}_1\cdot\vec{q}_3\vec{\sigma}_3\cdot\vec{q}_1\ \boldsymbol{\tau}_1\cdot\boldsymbol{\tau}_2\ S_3+\vec{\sigma}_1\cdot\vec{q}_1\vec{\sigma}_3\cdot\vec{q}_3\ \boldsymbol{\tau}_1\cdot\boldsymbol{\tau}_2\ S_4$$
$$+\vec{\sigma}_1\cdot\vec{q}_3\vec{\sigma}_3\cdot\vec{q}_3\ \boldsymbol{\tau}_1\cdot\boldsymbol{\tau}_2\ S_5+\vec{\sigma}_1\cdot\vec{\sigma}_3\ \boldsymbol{\tau}_1\cdot\boldsymbol{\tau}_2\ S_6$$
$$+\vec{q}_1\cdot\vec{q}_3\times\vec{\sigma}_1\ \boldsymbol{\tau}_1\cdot\boldsymbol{\tau}_2\times\boldsymbol{\tau}_3\ S_7, \tag{A6}$$

where the functions $S_i \equiv S_i(q_1, q_3, z)$ are given by

$$S_1 = -\frac{A(q_1)g_A^4\left(2M_\pi^2+q_1^2\right)}{128F^6\pi}-\frac{A(q_2)g_A^4\left(4M_\pi^2+q_1^2+zq_1q_3+q_3^2\right)}{128F^6\pi}-\frac{A(q_3)g_A^4\left(2M_\pi^2+q_3^2\right)}{128F^6\pi}$$
$$+\frac{I(4:0,-q_1,q_3;0)g_A^4\left(2M_\pi^2+q_1^2\right)\left(2M_\pi^2+q_3^2\right)}{32F^6}-\frac{g_A^4M_\pi}{64F^6\pi},$$
$$S_2 = -\frac{A(q_1)g_A^4((1+z^2)q_1+2zq_3)}{128F^6\pi(-1+z^2)^2q_1}-\frac{A(q_3)g_A^4q_3(2zq_1+(1+z^2)q_3)}{128F^6\pi(-1+z^2)^2q_1^2}$$
$$+\frac{I(4:0,-q_1,q_3;0)g_A^4q_3\left(-4z(-1+z^2)M_\pi^2+2zq_1^2+(1+3z^2)q_1q_3+2zq_3^2\right)}{32F^6(-1+z^2)^2q_1}$$
$$+\frac{A(q_2)g_A^4\left((1+z^2)q_1^2+z(3+z^2)q_1q_3+(1+z^2)q_3^2\right)}{128F^6\pi(-1+z^2)^2q_1^2},$$
$$S_3 = \frac{A(q_3)g_A^4((1+z^2)q_1+2zq_3)}{128F^6\pi(-1+z^2)^2q_1}+\frac{A(q_1)g_A^4(2zq_1+(1+z^2)q_3)}{128F^6\pi(-1+z^2)^2q_3}+\frac{zA(q_2)g_A^4\left(-2q_1^2+z(-5+z^2)q_1q_3-2q_3^2\right)}{128F^6\pi(-1+z^2)^2q_1q_3}$$
$$-\frac{I(4:0,-q_1,q_3;0)g_A^4\left(-4(-1+z^2)M_\pi^2+(1+z^2)q_1^2+z(3+z^2)q_1q_3+(1+z^2)q_3^2\right)}{32F^6(-1+z^2)^2},$$
$$S_4 = \frac{zA(q_1)g_A^4((1+z^2)q_1+2zq_3)}{128F^6\pi(-1+z^2)^2q_3}+\frac{zA(q_3)g_A^4(2zq_1+(1+z^2)q_3)}{128F^6\pi(-1+z^2)^2q_1}$$
$$+\frac{I(4:0,-q_1,q_3;0)zg_A^4\left(4z(-1+z^2)M_\pi^2-2zq_1^2-(1+3z^2)q_1q_3-2zq_3^2\right)}{32F^6(-1+z^2)^2}$$
$$-\frac{zA(q_2)g_A^4\left((1+z^2)q_1^2+z(3+z^2)q_1q_3+(1+z^2)q_3^2\right)}{128F^6\pi(-1+z^2)^2q_1q_3},$$
$$S_5 = -\frac{A(q_1)g_A^4q_1\left((1+z^2)q_1+2zq_3\right)}{128F^6\pi(-1+z^2)^2q_3^2}-\frac{A(q_3)g_A^4\left(2zq_1+(1+z^2)q_3\right)}{128F^6\pi(-1+z^2)^2q_3}$$
$$+\frac{I(4:0,-q_1,q_3;0)g_A^4q_1\left(-4z(-1+z^2)M_\pi^2+2zq_1^2+(1+3z^2)q_1q_3+2zq_3^2\right)}{32F^6(-1+z^2)^2q_3}$$

$$+\frac{A(q_2)g_A^4\left((1+z^2)q_1^2+z(3+z^2)q_1q_3+(1+z^2)q_3^2\right)}{128F^6\pi(-1+z^2)^2q_3^2},$$

$$S_6=-\frac{A(q_3)g_A^4q_3(zq_1+q_3)}{128F^6\pi(-1+z^2)}+\frac{A(q_2)g_A^4\left(q_1^2-z(-3+z^2)q_1q_3+q_3^2\right)}{128F^6\pi(-1+z^2)}-\frac{A(q_1)g_A^4q_1(q_1+zq_3)}{128F^6\pi(-1+z^2)}$$
$$+\frac{I(4:0,-q_1,q_3;0)g_A^4q_1q_3(zq_1+q_3)(q_1+zq_3)}{32F^6(-1+z^2)},$$

$$S_7=\frac{A(q_1)g_A^4\left(2M_\pi^2+q_3^2\right)}{256F^6\pi(-1+z^2)q_3^2}-\frac{A(q_2)g_A^4\left(zq_3^2(zq_1+q_3)+2M_\pi^2(q_1+zq_3)\right)}{256F^6\pi(-1+z^2)q_1q_3^2}+\frac{zA(q_3)g_A^4\left(2M_\pi^2+q_3^2\right)}{256F^6\pi(-1+z^2)q_1q_3}$$
$$-\frac{I(4:0,-q_1,q_3;0)g_A^4(zq_1+q_3)\left(2M_\pi^2+q_3^2\right)}{64F^6(-1+z^2)q_3}. \tag{A7}$$

Examining these results one observes that the individual terms in the expressions for R_i and S_i are singular for $z=\pm1$, $q_1=0$, and/or $q_3=0$. These singularities, however, cancel in such a way that the resulting terms in Eqs. (A1) and (A6) are finite. In principle, it is possible to obtain a representation for functions R_i and S_i that is free of at least some of the singularities. In particular, the singularities at $z=\pm1$ can be avoided if one expresses the results in terms of the functions J_1 and J_2 defined as

$$J_1(d,\vec{q}_1,\vec{q}_3)$$
$$=\frac{1}{1-z^2}\left\{J(d:\vec{0},-\vec{q}_1,\vec{q}_3)-\frac{1}{2}(1+z)\right.$$
$$\times\left[\frac{J(d:\vec{0},\vec{q}_1)}{q_3^2+q_1q_3}+\frac{J(d:\vec{0},\vec{q}_3)}{q_1^2+q_1q_3}-\frac{J(d:\vec{0},\vec{q}_1+\vec{q}_3)}{q_1q_3}\right]$$
$$-\frac{1}{2}(1-z)\left[\frac{J(d:\vec{0},\vec{q}_1)}{q_3^2-q_1q_3}+\frac{J(d:\vec{0},\vec{q}_3)}{q_1^2-q_1q_3}\right.$$
$$\left.\left.+\frac{J(d:\vec{0},\vec{q}_1+\vec{q}_3)}{q_1q_3}\right]\right\}, \tag{A8}$$

$$J_2(d,\vec{q}_1,\vec{q}_3)$$
$$=\frac{1}{(1-z^2)^2}\left\{J(d:\vec{0},-\vec{q}_1,\vec{q}_3)-\frac{1}{4}(1-z)^2\right.$$
$$\times\left[\frac{J(d:\vec{0},\vec{q}_1)}{q_3^2-q_1q_3}+\frac{J(d:\vec{0},\vec{q}_3)}{q_1^2-q_1q_3}+\frac{J(d:\vec{0},\vec{q}_1+\vec{q}_3)}{q_1q_3}\right.$$
$$+(1+z)\left[-\frac{8M^2-2q_1^2+(d-1)(q_1-q_3)(2q_1-q_3)}{(d-1)q_3(q_1-q_3)^3}\right.$$
$$\times J(d:\vec{0},\vec{q}_1)$$
$$+\frac{8M^2-2q_3^2+(d-1)(q_1-q_3)(q_1-2q_3)}{(d-1)q_1(q_1-q_3)^3}J(d:\vec{0},\vec{q}_3)$$
$$\left.+\frac{2(4M^2+(d-2)(q_1-q_3)^2)}{(d-1)q_1q_3(q_1-q_3)^2}J(d:\vec{0},\vec{q}_1+\vec{q}_3)\right]\Big]$$
$$-\frac{1}{4}(1+z)^2\left[\frac{J(d:\vec{0},\vec{q}_1)}{q_3^2+q_1q_3}+\frac{J(d:\vec{0},\vec{q}_3)}{q_1^2+q_1q_3}\right.$$
$$\left.-\frac{J(d:\vec{0},\vec{q}_1+\vec{q}_3)}{q_1q_3}\right.$$
$$+(1-z)\left[\frac{8M^2-2q_1^2+(d-1)(q_1+q_3)(2q_1+q_3)}{(d-1)q_3(q_1+q_3)^3}\right.$$
$$\times J(d:\vec{0},\vec{q}_1)$$
$$+\frac{8M^2-2q_3^2+(d-1)(q_1+q_3)(q_1+2q_3)}{(d-1)q_1(q_1+q_3)^3}$$
$$\times J(d:\vec{0},\vec{q}_3)$$
$$\left.\left.\left.-\frac{2(4M^2+(d-2)(q_1+q_3)^2)}{(d-1)q_1q_3(q_1+q_3)^2}J(d:\vec{0},\vec{q}_1+\vec{q}_3)\right]\right]\right\}, \tag{A9}$$

rather than the three-point function $J(d:\vec{0},-\vec{q}_1,\vec{q}_3)$ and uses certain linear combinations of two-point functions and tadpole integrals. In these expressions, the two-point function is defined as

$$J(d:\vec{p}_1,\vec{p}_2)=\int\frac{d^dl}{(2\pi)^d}\frac{1}{(\vec{l}+\vec{p}_1)^2+M_\pi^2}\frac{1}{(\vec{l}+\vec{p}_2)^2+M_\pi^2}. \tag{A10}$$

[1] N. Kalantar-Nayestanaki and E. Epelbaum, Nucl. Phys. News **17**, 22 (2007).
[2] D. R. Entem and R. Machleidt, Phys. Rev. C **68**, 041001(R) (2003).
[3] E. Epelbaum, W. Glöckle, and U.-G. Meißner, Nucl. Phys. **A747**, 362 (2005).
[4] S. Weinberg, Phys. Lett. **B251**, 288 (1990).
[5] S. Weinberg, Nucl. Phys. **B363**, 3 (1991).
[6] U. van Kolck, Phys. Rev. C **49**, 2932 (1994).
[7] J. L. Friar, D. Huber, and U. van Kolck, Phys. Rev. C **59**, 53 (1999).
[8] E. Epelbaum, A. Nogga, W. Glöckle, H. Kamada, Ulf-G. Meißner, and H. Witala, Phys. Rev. C **66**, 064001 (2002).
[9] E. Epelbaum, Prog. Part. Nucl. Phys. **57**, 654 (2006).

[10] A. Nogga, P. Navratil, B. R. Barrett, and J. P. Vary, Phys. Rev. C **73**, 064002 (2006).
[11] P. Navratil, V. G. Gueorguiev, J. P. Vary, W. E. Ormand, and A. Nogga, Phys. Rev. Lett. **99**, 042501 (2007).
[12] J. Ley *et al*., Phys. Rev. C **73**, 064001 (2006).
[13] Y. Koike and J. Haidenbauer, Nucl. Phys. **A463**, 365 (1987).
[14] H. Witała, D. Hüber, and W. Glöckle, Phys. Rev. C **49**, R14 (1994).
[15] S. Ishikawa and M. R. Robilotta, Phys. Rev. C **76**, 014006 (2007).
[16] S. C. Pieper, V. R. Pandharipande, R. B. Wiringa, and J. Carlson, Phys. Rev. C **64**, 014001 (2001).
[17] S. A. Coon and J. L. Friar, Phys. Rev. C **34**, 1060 (1986).
[18] M. R. Robilotta, Phys. Rev. C **74**, 044002 (2006); **74**, 059902(E) (2006).
[19] J.-I. Fujita, M. Kawai, and M. Tanifuji, Nucl. Phys. **29**, 252 (1962).
[20] N. Fettes, U.-G. Meißner, and S. Steininger, Nucl. Phys. **A640**, 199 (1998).
[21] V. Bernard, Prog. Part. Nucl. Phys. **60**, 82 (2007).
[22] E. Epelbaum, U.-G. Meißner, and W. Glöckle, Nucl. Phys. **A714**, 535 (2003).
[23] E. Epelbaum, Phys. Lett. **B639**, 456 (2006).
[24] E. Epelbaum, Eur. Phys. J. A **34**, 197 (2007).
[25] V. Bernard, N. Kaiser, and U.-G. Meißner, Nucl. Phys. **A615**, 483 (1997).